Supplementary Information

Biological manganese oxidation in biofilms from oxygen-supplemented biological activated carbon (BAC) filters

Amanda Larasati[a,∞], Olga Bernadet[a,b,∞], Gert Jan W. Euverink[b], H. Pieter J. van Veelen[a] and Maria Cristina Gagliano[a*]

[a] Wetsus, Center of European Excellence in Water Technology, Oostergoweg 9, 8911 MA, Leeuwarden, The Netherlands

[b] Engineering and Technology Institute Groningen (ENTEG), University of Groningen, Nijenborgh 4, Groningen, The Netherlands

*Corresponding author: M. Cristina Gagliano cristina.gagliano@wetsus.nl

[∞] Amanda Larasati and Olga Bernadet contributed equally to this article.

Figures

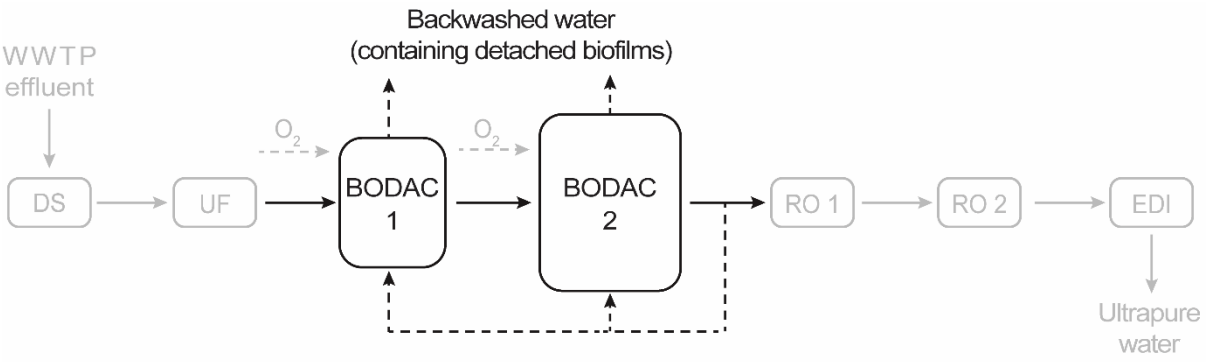

Figure S1 - Schematic overview of the water treatment line at the Ultrapure water (UPW) factory in Emmen, the Netherlands. The biological activated carbon (BAC) filters are named biological oxygen-dosed activated carbon (BODAC) since they are operated with pure oxygen dosed to the system to maintain aerobic conditions and stimulate biodegradation. DS: Drum sieve (opening size 1 mm), UF: Ultrafiltration (pore size 0.04 μm), RO: Reverse osmosis, EDI: Electrodeionization, and WWTP: Wastewater treatment plant. The scheme is derived from Bernadet et al. (2023).

Description for Figure S1

The BODAC filters comprise two consecutive BAC filters, BODAC 1 and 2, where oxygen is dosed at their influent. The influent of BODAC 1 comprised ultrafiltration (UF) permeate, while BODAC 2 influent consisted of the effluent of BODAC 1. The empty bed contact time (EBCT) of BODAC 1 and 2 are 16 and 32 min, respectively (van der Maas et al., 2020). The oxygen consumption in these BAC filters varied between 5 – 40 mg O_2 L^{-1} (van der Maas et al., 2009). Periodical backwashing with air and water (from BODAC 2 effluent) is applied to decrease pressure build-up due to the accumulation of (bio)solids and to avoid excess biofilm growth.

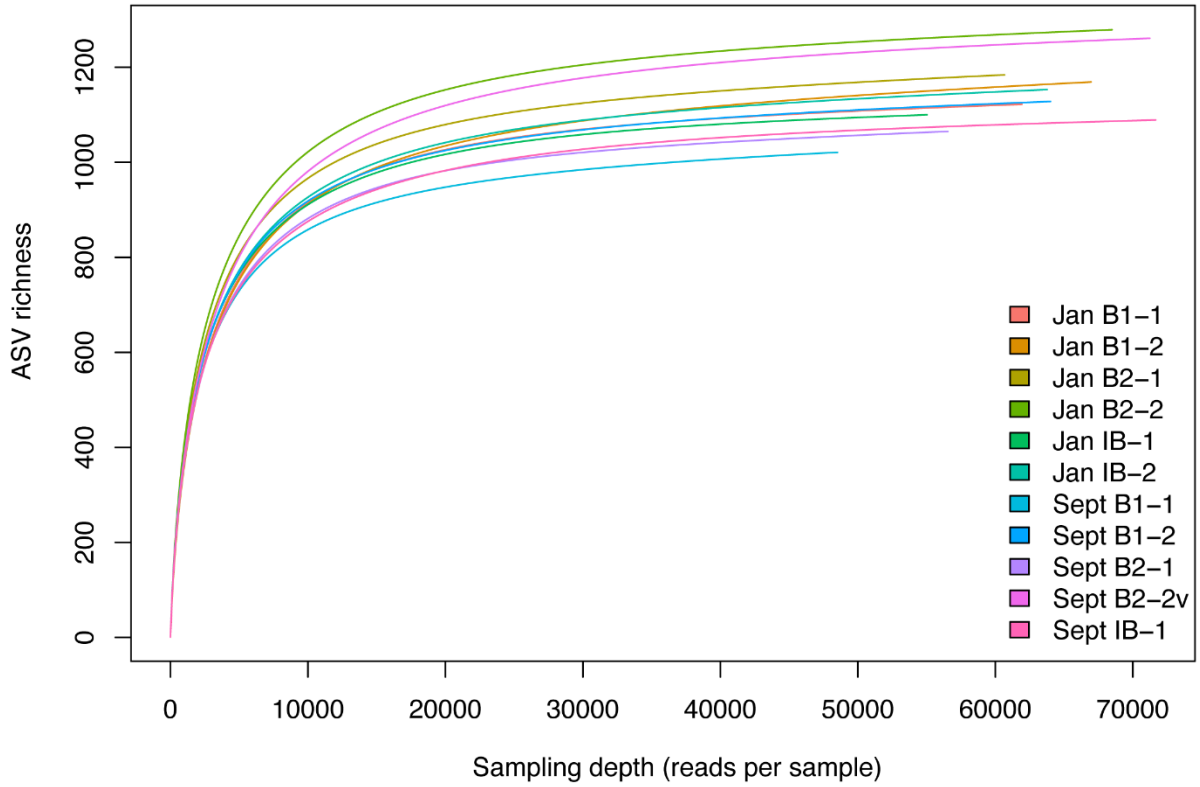

Figure S2 - Rarefaction curves based on amplicon sequence variants (ASVs) accumulation as a function of sequencing sampling depth, demonstrating plateaus for all curves of different samples. Each curve represents one individual sample (for Sept and Jan, inoculum biofilm (IB) and the two bottle replicates (B1 and B2)).

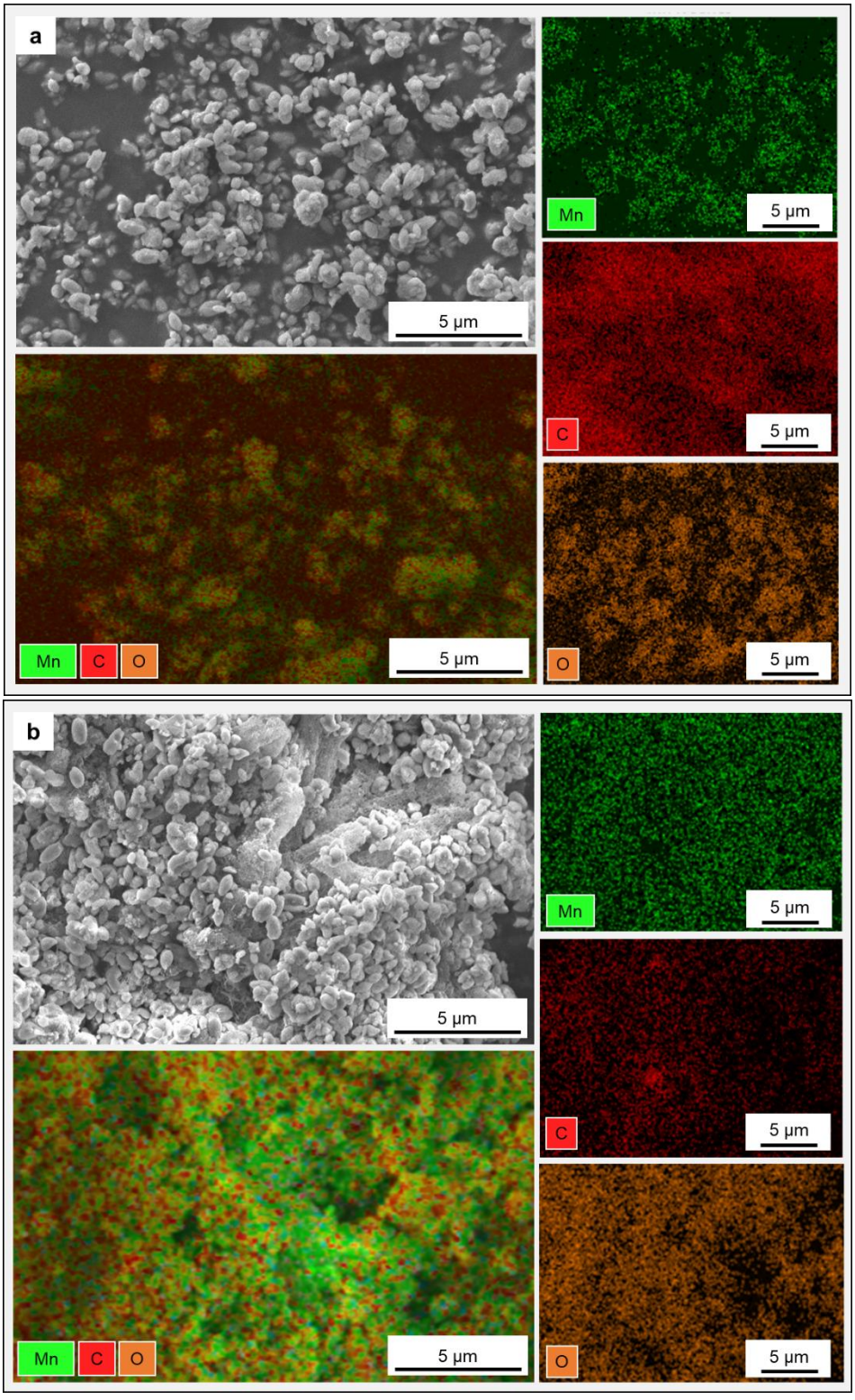

Figure S3 – The most abundant elements (≥ 1 %) manganese (Mn), carbon (C), and oxygen (O), measured by the Energy Dispersive X-Ray (EDX) analysis on the raw $MnCO_3$ slurry (a) and the non-active (control) biofilms at the end of the 42-days experiment (b).

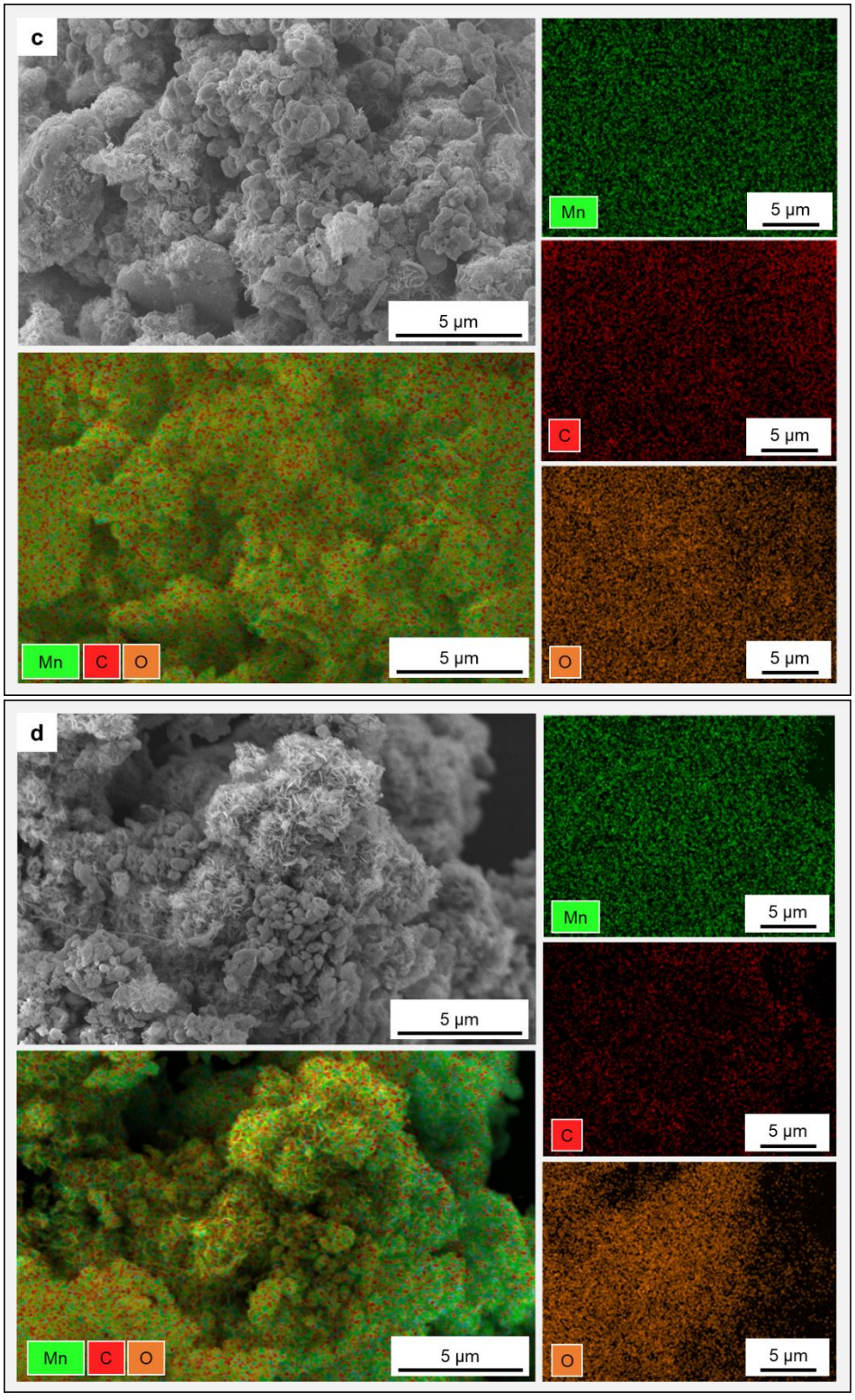

Figure S3 *(Continued)* – The most abundant elements (≥ 1 %) manganese (Mn), carbon (C), and oxygen (O), measured by the Energy Dispersive X-Ray (EDX) analysis on the active biofilms from September (c) and January bottles (d) at the end of 42-days incubation.

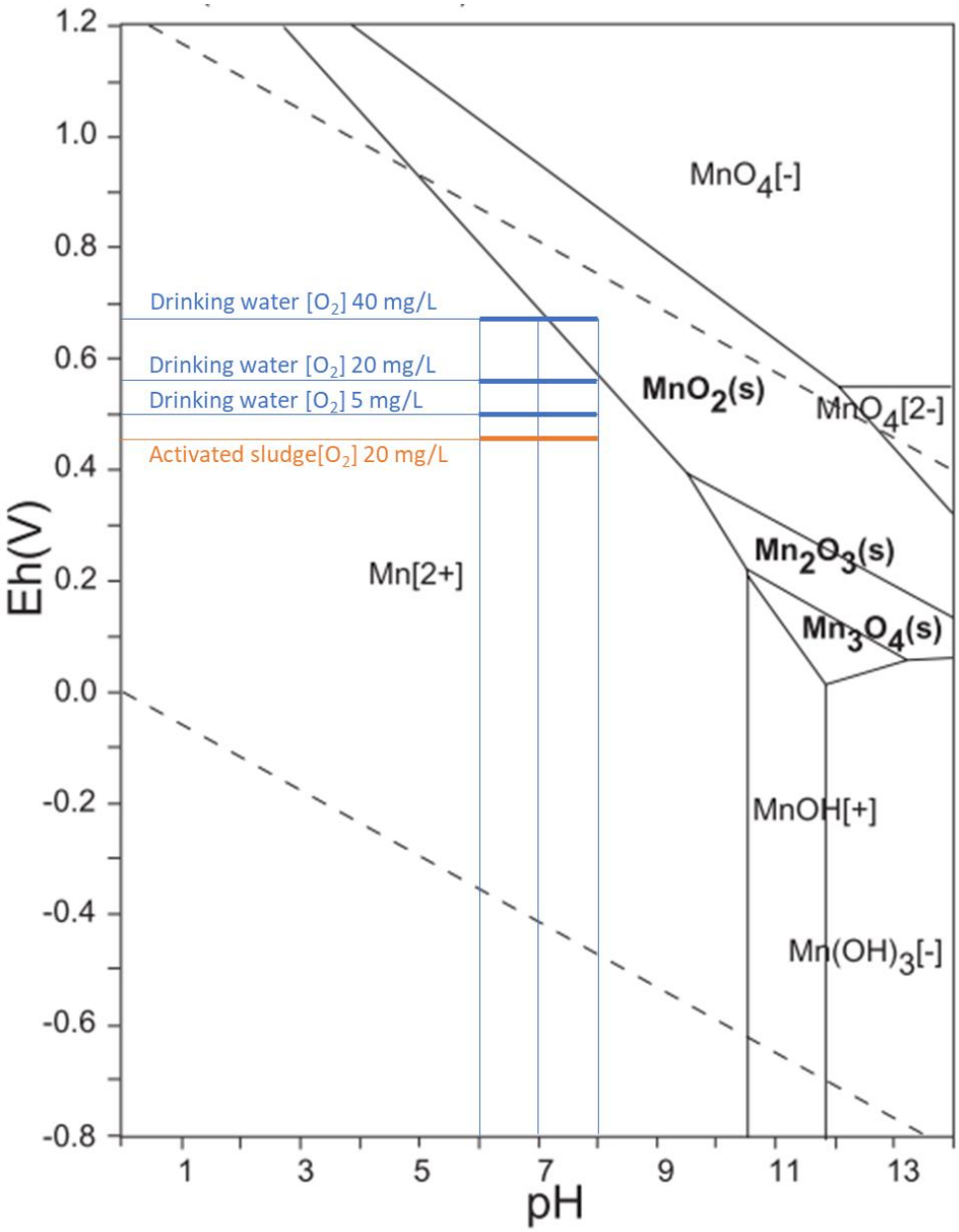

Figure S4 – Pourbaix diagram for manganese, adapted from Takeno, 2005 to include values for drinking water and activated sludge.

Description for Figure S4

As mentioned in the description for Figure S1, the BODAC filters were dosed with pure oxygen, and the oxygen consumption in the filters ranged from 5 to 40 mg O_2 L^{-1} (van der Maas et al., 2009). We estimated the redox potential (Eh) based on the dissolved oxygen

concentration [O_2] in the system. Initially, we estimated the Eh in activated-sludge reactors condition at pH 7 (Heduit and Thevenot, 1989).

1. [O_2] = 5 mg L^{-1}, Eh = 0.46
2. [O_2] = 15 mg L^{-1}, Eh = 0.47
3. [O_2] = 40 mg L^{-1}, Eh = 0.50

As a comparison in a drinking water system, the maximum Eh values obtained with dissolved oxygen concentration at 8 mg L^{-1} and pH 7 was around 0.59 and increased steadily by approximately 0.005 with every increase of 1 mg L^{-1} of dissolved oxygen concentration (James et al., 2004). It can be estimated that the redox potential in drinking water when dissolved oxygen concentrations 5, 15, and 40 mg L^{-1} are 0.51, 0.56, and 0.68, respectively. These values can be lower in the inlet of BODAC filters because the redox potential is not solely affected by the oxygen concentration but also by the presence of organic matter, the salinity of the water, and temperature.

A

	Phylum	IB	B1	B2
	Proteobacteria	21.9	39.8	41.4
	Planctomycetota	8.5	10.9	9.9
	Bacteroidota	19.9	3.2	3.8
	Acidobacteria	7.3	4.3	5.1
	Nitrospirota	4.8	3.1	1.6
	Actinobacteriota	0.2	2.4	3.8
	Class/Order	**IB**	**B1**	**B2**
Proteobacteria	Class *Alphaproteobacteria*	12.5	17.4	17.1
	Order *Rhizobiales*	5.5	12.4	12.8
	Order *Sphingomonadales*	4.1	1.7	1.7
	Class *Gammaproteobacteria*	9.4	22.4	24.3
	Order *Burkholderiales*	8.6	20.1	22.2
Bacteroidota	Class *Bacteroidia*	19.9	3.2	3.8
	Order *Chitinophagales*	15.5	3.1	3.7
	Order *Flavobacteriales*	4.4	0.1	0.1

B

	Phylum	IB	B1	B2
	Proteobacteria	20.2	46.3	44.4
	Planctomycetota	6.1	7.9	9.0
	Bacteroidota	26.4	10.1	5.5
	Acidobacteriota	5.2	4.1	3.8
	Nitrospirota	5.6	1.4	1.4
	Actinobacteriota	0.1	1.4	1.9
	Class/Order	**IB**	**B1**	**B2**
Proteobacteria	Class *Alphaproteobacteria*	9.9	19.7	21.7
	Order *Rhizobiales*	3.7	16.0	17.6
	Order *Sphingomonadales*	3.4	1.1	1.2
	Class *Gammaproteobacteria*	10.3	26.6	22.7
	Order *Burkholderiales*	9.3	14.1	13.9
Bacteroidota	Class *Bacteroidia*	26.4	10.1	5.5
	Order *Chitinophagales*	21.8	10.0	5.4
	Order *Flavobacteriales*	4.5	0.1	0.1

Figure S5 – Relative abundances of the main phyla, classes and orders of the domain *Bacteria* identified into the inoculum biofilm (IB) sampled in September (in A) and January (in B) for each of the duplicate experimental cultures analyzed via 16S rRNA gene amplicon sequencing (B1 and B2).

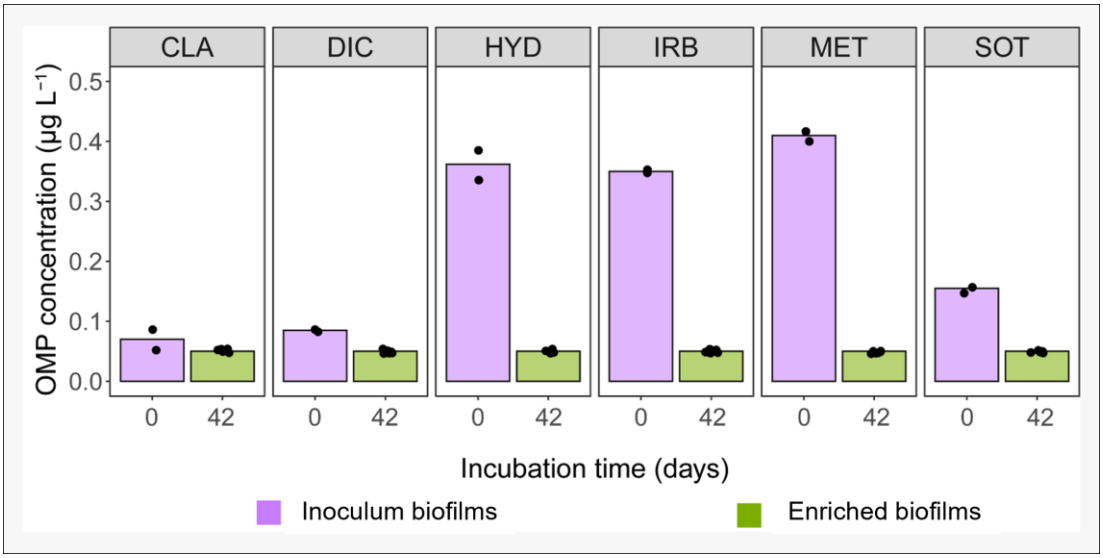

Figure S6 – Decrease in concentration of relevant organic micropollutants (OMPs) along 42 days in the enrichment experiment of September. As also shown by the SEM and XRD analyses, the inoculum biofilms (day 0) did not contain δ-MnO_2 (birnessite), while the enriched biofilms (day 42) contained a high amount of crystalline δ-MnO_2.

OMPs concentration was determined in duplicate samples by liquid chromatography – mass spectrometry (LC-MS), following the method described in Bernadet et al., (2023).

CLA: clarithromycin, DIC: diclofenac, HYD: hydrochlorothiazide, IRB: irbesartan, MET: metoprolol, SOT: sotalol.

Tables

Table S1 – Analysis of water samples harvested to collect the inoculum biofilms from the BAC filters during the two campaigns in September 2021 and January 2022 (n = 2).

Parameter	September 2021			January 2022		
tCOD (mg/L)	89	±	5.44	50.6	±	1.82
tN (mg N/L)	10.6	±	1.32	9.46	±	1.33
tP (mg P/L)	0.87	±	0	0.21	±	0.07
Cations						
Ca^{+} (mg/L)	32	±	0.35	31.1	±	0.14
Na^{+} (mg/L)	61	±	0.3	52.1	±	0.14
NH_4^{+} (mg N/L)	<0.1			1.87	±	0.07
Anions						
Cl^{-} (mg/L)	134	±	0.41	71.2	±	0.29
NO_2^{-} (mg N/L)	<0.1			0.64	±	0.01
NO_3^{-} (mg N/L)	6.53	±	0.2	4.83	±	0.03
PO_4^{3-} (mg/L)	0.39	±	0.02	0.42	±	0.02
SO_4^{2-} (mg/L)	> 80			37.9	±	0.21
Element						
Fe (mg/L)	0.046	±	0.0089	0.058	±	0.0016
Mn (mg/L)	6.1	±	0.2	2.0	±	0.1
Zn (mg/L)	0.12	±	0.001	0.003	±	0.0002
Al (mg/L)	1.1	±	0.01	0.046	±	0.0003

Materials and Methods for Table S1

- *Total chemical oxygen demand, nitrogen, and phosphate*

Total chemical oxygen demand (tCOD) and total nitrogen (tN), and total phosphate (tP) were determined using Hach Lange cuvette tests (Hach Lange, US): LCK 314 for tCOD, LCK 138 for tN, and LCK 349 for tP following the manufacturer's instructions. The sample volume required for each replicate measurement for tCOD, tN, and tP was 2, 1.3, and 2 mL, respectively.

- *Cations, anions, and elements measurement*

Cations and anions were determined in the soluble fraction of the water samples, filtered using 0.45 μm PFTE filters. Cations (NH_4^+, Ca^{2+}, and Na^+) were measured using Ion chromatograph Compact IC Flex 881 and Compact IC Flex 930 (Metrohm AG, CH) equipped with a Metrosep C4 – 150/4.0 mm column (Metrohm AG) and 3 mM nitric acid as the mobile phase. The injection volume of the sample was 100 μL. Anions (Cl^-, NO_2^-, NO_3^-, PO_4^{3-}, and SO_4^{2-}) were measured using Ion Chromatograph Compact IC 761 (Metrohm AG) using a Metrosep A Supp 5, 150/4.0 mm column. The first mobile phase consisted of 3.2 mM sodium carbonate, 1 mM sodium bicarbonate, and 1% (v/v) acetone. The second mobile phase consisted of 0.5 mM orthophosphoric acid and 1% (v/v) acetone. The injection volume of the sample was 20 μL.

Elements were measured using Optima 5300 DV Inductively Coupled Plasma Optical Emission Spectroscopy (ICP-OES) (Perkin Elmer, US) with argon as the carrier gas. An internal standard of Yttrium (Y) (Fluka, CH) was used.

Table S2 - Evaluation of the Mn speciation measurement with Inductively Coupled Plasma Optical Emission Spectroscopy (ICP-OES).

Salt	Supplier	Average Mn oxidation state	Mn acid-soluble fraction (mmol/L)	Mn acid-insoluble fraction (mmol/L)	Mn total (mmol/L)	Mn acid-soluble fraction (%)	Mn acid-insoluble fraction (%)
$MnCl_2.4H_2O$	Sigma Aldrich #M3634	2	1.9	0.02	1.92	98.9%	1.1%
$MnCO_3$	Alfa Aesar #14344	2	1.72	0.02	1.74	98.6%	1.4%
Mn_3O_4	Sigma Aldrich #377473	2.7	0.99	1.07	2.06	47.9%	52.1%
MnO_2	Sigma Aldrich #805958	4	0.06	2.41	2.47	2.4%	97.6%

Materials and Methods for Table S2

Manganese oxidation state characterization

For the ICP-OES method development, four Mn salts were used as reference, based on their Mn oxidation state and the solubility of Mn species when in acid, which was added as 1 M nitric acid (HNO_3). The Mn(II) from manganese chloride ($MnCl_2$) and manganese carbonate ($MnCO_3$) should be soluble or become soluble when in the acid. The Mn from manganese oxide (Mn_3O_4) should be partially soluble as Mn is present in both oxidation states Mn(II) and Mn(III), while the Mn(IV) in manganese dioxide (MnO_2) should not be soluble in the acid, but only become soluble after microwave digestion using a combination of HNO_3 and hydrogen peroxide (H_2O_2) (Characteristic Reactions of Manganese (Mn^{2+}), 2020 and Neaman et al., 2004).

References

Bernadet, O., Larasati, A., Van Veelen, H.P.J., Euverink, G.J.W., Gagliano, M.C., 2023. Biological Oxygen-dosed Activated Carbon (BODAC) filters – A bioprocess for ultrapure water production removing organics, nutrients and micropollutants. Journal of Hazardous Materials 458, 131882. https://doi.org/10.1016/j.jhazmat.2023.131882

Heduit, A., Thevenot, D., 1989. Relation between redox potential and oxygen levels in activated-sludge reactors. Water Science and Technology 21, 947–956.

James, C.N., Copeland, R.C., Lytle, D.A., 2004. Relationships Between Oxidation-Reduction Potential, Oxidant, and pH in Drinking Water. Presented at the American Water Works Association Water Quality and Technology Conference.

Neaman, A., Waller, B., Mouélé, F., Trolard, F., Bourrié, G., 2004. Improved methods for selective dissolution of manganese oxides from soils and rocks. European Journal of Soil Science 55, 47–54. https://doi.org/10.1046/j.1351-0754.2003.0545.x

Takeno, N., 2005. Atlas of Eh-pH diagrams Intercomparison of thermodynamic databases. National Institute of Advanced Industrial Science and Technology Tokyo 285.

van der Maas, P., Majoor, E., Schippers, J.C., 2009. Biofouling Control by Biological Activated Carbon Filtration: a Promising Method for WWTP Effluent Reuse, in: IWA Membrane Technology Conference. Presented at the IWA Membrane Technology Conference, Beijiing, China.

van der Maas, P., Veenendaal, G., Nonnekens, J., Brink, H., de Vogel, D., 2020. Biologische actiefkoolfiltratie met zuurstofdosering: veelbelovende techniek voor verwijdering geneesmiddelen? H2O/Waternetwerk.

Chemistry LibreTexts. 2020. Characteristic Reactions of Manganese (Mn^{2+}). [online] Available at: https://chem.libretexts.org/Bookshelves/Analytical_Chemistry/Supplemental_Modules_(Analytical_Chemistry)/Qualitative_Analysis/Characteristic_Reactions_of_Select_Metal_Ions/Characteristic_Reactions_of_Manganese_Ions_(Mn%C2%B2%E2%81%BA)> (Accessed 20 June 2022).